Journal of Applied Polymer Science

Acrylic bone cements modified with poly(ethylene glycol)-based biocompatible phase-change materials

Klaudia Król, Beata Macherzyńska, Kinga Pielichowska
Faculty of Materials Science and Ceramics, Department of Biomaterials, AGH University of Science and Technology, Kraków 30-059, Poland
Correspondence to: K. Pielichowska (E-mail: kingapie@agh.edu.pl)

ABSTRACT: The high polymerization temperature of acrylic bone cements used in hip replacement implantation may cause thermal necrosis of surrounding tissues. In order to reduce the polymerization temperature, acrylic bone cement has been modified with a biocompatible polymeric phase-change material (PCM) based on poly(ethylene glycol) (PEG) of different molecular weights and stabilized with potato starch. Structural and morphological studies were performed, and the thermal and mechanical properties were investigated. The incorporation of PEG-based PCM led to a decrease in the polymerization temperature of bone cement from 70 °C for unmodified cement to 58 °C for modified cement. Modified cement materials were stable in incubation tests, although acoustic analysis data revealed a decrease in propagation speed after incubation, which indicates formation of material defects (pores, cracks, voids, etc.) due to water activity. However, in the regeneration process, these defects can be filled by freshly grown bone tissue leading to better incorporation of bone cement replacements into tissue. © 2016 Wiley Periodicals, Inc. J. Appl. Polym. Sci. **2016**, *133*, 43898.

KEYWORDS: biomaterials; differential scanning calorimetry (DSC); polysaccharides; thermal properties

Received 12 January 2016; accepted 5 May 2016
DOI: 10.1002/app.43898

INTRODUCTION

Acrylic bone cements have been commonly used as polymeric biomaterial,[1] and their main function is to anchor the joint prosthesis to the bone interior.[2] The space between the implant and the bone is filled with cement,[3] which is an interface between the stiff metal prosthesis and the more flexible hard tissue.[4] This biomaterial is also the most popular bone substitute used to treat spinal fractures in vertebroplasty procedures.[5]

Acrylic bone cements based mainly on poly(methyl methacrylate) (PMMA) have been used in total joint arthroplasty since Sir John Charnley developed his low-friction arthroplasty of the hip in the late 1950s.[6,7] These cements were composed of cold-polymerized PMMA, which reached the final setting *in situ* and can be an elastic buffer, maintaining the prosthesis in place and transferring the load from the prosthesis to the bone. Since then, little has changed in the composition of commercially available acrylic bone cements. Commercially available acrylic bone cements comprise of PMMA powder and methyl methacrylate (MMA) liquid.[8] The powder phase consists of pre-polymerized PMMA, the initiator benzoyl peroxide (BPO), and radiopaque components (e.g., ZrO_2).[9] The liquid composes of MMA monomer, *N*,*N*-dimethyl-*p*-toluidine (DMPT) as a polymerization activator and hydroquinone (HQ)[10] as a polymerization inhibitor. These two phases are mixed and then can be inserted into the bone interior.[11]

PMMA bone cement is characterized by relatively high mechanical strength, a suitable curing time, and ease of application. However, some drawbacks of the polymerization process of bone cement have been identified. The main problem is the high temperature reached during the curing process, which range from 40 °C to 110 °C.[12] The long exposure of living tissue to high temperatures can lead to extensive bone damage.[13,14]

Many attempts have been made to reduce the high polymerization temperature of acrylic bone cements. Pascual *et al.*[15] obtained a new bone cement by the partial replacement of MMA with a higher molar mass and more hydrophilic monomer, ethoxytriethyleneglycol methacrylate (TEG). Addition of TEG to the bone cement composition caused a reduction in the maximum temperature and an elongation of the setting time. However, the mechanical properties, such as the Young's modulus and the ultimate tensile strength, of the modified cement were decreased.[15] In the work by Ormsby *et al.*,[16] acrylic bone cement was modified with multi-walled carbon nanotubes (MWCNT). The addition of MWCNT allowed for reduction in the maximum temperature during polymerization, but the setting time was significantly elongated, depending on the MWCNT content.[16] MWCNT application for biomedical

Table I. Compositions and thermal properties of PEG/Starch Systems

Sample	Composition (80:20 wt/wt)	T_{onset} (°C)	T_{endset} (°C)	ΔH_m (J/g)	ΔH_m/PEG (J/g)	X_c (%)
PEG2S	PEG 2000/starch	36.13	60.94	127.44	159.30	80.95
PEG3S	PEG 3000/starch	48.11	65.29	139.99	174.99	88.92
PEG4S	PEG 4000/starch	48.95	68.45	142.13	177.66	90.28
PEG6S	PEG 6000/starch	51.94	69.28	139.56	174.45	88.64
PEG8S	PEG 8000/starch	52.26	69.44	146.82	183.53	93.25
PEG10S	PEG 10,000/starch	52.93	68.78	133.00	166.25	84.48
PEG12S	PEG 12,000/starch	54.75	70.77	149.93	187.41	95.23

DSC data for PEG/starch systems: the onset temperature (T_{onset}), the endset temperature (T_{endset}), heat of phase transition (ΔH_m), heat of phase transition of 100% PEG (ΔH_m/PEG), and degree of crystallinity (X_c) of PEG in PEG/starch systems

purposes requires special attention since there are numerous indications of toxicity and detrimental effects on DNA.[17]

Another way to reduce the high polymerization temperature is by using phase-change materials (PCMs) that act as thermal energy storage systems. To minimize the high polymerization temperature, De Santis *et al.*[18] prepared a blend of PMMA and PMMA with encapsulated paraffin-based PCM.[19] However, the bending strength decreased from 66 MPa for unmodified cement to 44 MPa for the cement modified with about 12 wt % PCM.

Generally, PCMs can be used for the storage of thermal energy in the form of sensible and latent heat.[20] In the present study, poly(ethylene glycol) (PEG) was applied as a PCM to decrease the temperature of polymerization of acrylic bone cement.

PEG shows a number of advantages as an energy-storage material: it is a biocompatible polymer that is used in drug applications,[21] and the melting range of PEG and the polymerization temperature of acrylic bone cement are comparable. However, the main problem with using PEG as a PCM is its melting during the phase transition, which can lead to the leakage of PEG from the bone cement, and, in consequence, the mechanical strength of the bone cement is reduced. To prevent PEG leakage, PEG can be shape stabilized using, for example, potato starch. In our previous work,[22] it was possible to obtain PEG-based system with a solid–solid phase transition through gelatinization of potato starch in an aqueous solution of PEG. Potato starch links PEG in the spatial network, and therefore, PEG cannot leak even above its melting point due to hydrogen bonding with amylose and amylopectin chains. Potato starch can be used as a shape stabilizer of PEG in biomedical applications as a natural, non-toxic, safe polymer. Additionally, starch can undergo gelatinization in the presence of PEG, which leads to formation of hydrogen bonds between starch and PEG macrochains.[22] As a result, shape-stabilized PEG/starch phase-change materials can be obtained.

In this work, acrylic bone cement was modified with PEG PCM of different molecular weights and stabilized with potato starch according to our patent application.[23] The influence of PCM introduction on the polymerization temperature, curing process, and acrylic bone properties was investigated.

EXPERIMENTAL

Materials

Duracryl®Plus, an acrylic bone cement (denture base resin) was purchased from Spofa Dental (Czech Republic). PEG (Sigma-Aldrich, Germany) with average molecular weights of 2000, 3000, 4000, 6000, 8000, 10,000 and 12,000 g/mol was used as a cement modifier. Potato starch (POCH S.A., Poland) was added to the PEG as a shape stabilizer.

Preparation of PEG/Starch Systems

Initially, shape-stabilized phase-change materials (SSPCM, PEG/starch systems) were prepared. Based on our previous work,[22] we used the PEG/starch ratio of 80/20 wt/wt regardless of the molar mass of PEG, because at this ratio maximal PEG content could be reached without PEG leakage. PEG (8 g) of a given molecular weight was dissolved in 90 mL of distilled water, and then 2 g of potato starch was dispersed in the prepared solution. The mixture was placed in a water bath at 72 °C and stirred for 5–7 min. When the mixture was gelatinized, the solution was poured into a Petri dish and dried at room temperature for 7 days. The composition of prepared SSPCM is given in Table I.

Acrylic bone cement was modified with 15% SSPCM. To form a suitable bone cement paste, the ratio of solid-phase to liquid-phase (m/vol) was 1 g of powder to 0.37 mL of liquid. Additionally, 0.15 g SSPCM was added to the cement powder. All components were put into a polyethylene container and mixed for 1.5 min. Setting time was measured for a system containing 1.5 g PMMA powder, 0.3 g PEG/starch modifier, and 0.555 mL MMA liquid. After mixing, the bone cement paste was placed into the Teflon mold. Temperature was measured for 1.5 g of cement powder. The cement paste was put into the polyethylene containers where the electronic thermometer was inserted.

Methods

For the differential scanning calorimetry (DSC) measurements, a Mettler-Toledo DSC 1 operating in dynamic and isothermal mode was employed. The conditions for dynamic measurements were: samples of about 4.5 mg, heating/cooling rate of 10 K/min, a nitrogen atmosphere, and an intracooler was used for cooling. For isothermal measurements: samples of about 10 mg,

temperature 20 °C for 15 min, and a nitrogen atmosphere with a flow rate of 30 mL/min.

Infrared spectra of the samples were recorded under vacuum at room temperature in KBr pellets using a Vertex 70v (Bruker) Fourier-transform infrared spectrometer (FTIR) in the range 4000–550 cm^{-1} at a resolution of 2 cm^{-1}.

A scanning electron microscope (SEM; Nova Nano SEM 200), equipped with an energy dispersive X-ray analyzer (Link ISIS-EDX), was used to investigate the surface microstructure of carbon-coated samples with an electron beam energy of 5 kV.

Thermogravimetric (TG) analysis was performed using a NETZSCH STA 449 F3 Jupiter® thermal analyzer, operating in a dynamic mode at a heating rate of 10 K/min under the following conditions: sample weight, about 12 mg; nitrogen atmosphere; sealed aluminium pan.

The Gillmore Needle Method of testing for the initial and final setting time of acrylic cement was used. This test was conducted according to the ASTM C266-99 standard.[24] The curing parameters (maximum temperature T_{max} and setting time t_{set}) were measured in accordance with the ISO 5833 standard. The temperature was measured using an electronic thermometer inside the polyethylene mold. Based on the above measurements, the curing profiles were plotted and the maximum polymerization temperature (T_{max}) was determined. The curing temperature was calculated using eq. (1):

$$T_{cure} = (T_{max} + T_{amb})/2 \quad (1)$$

where: T_{cure} = curing temperature, T_{max} = maximum temperature, and T_{amb} = ambient temperature.

Samples were incubated at 37 °C according to EN ISO 10993-13 for 3 months in distilled water. The pH, conductivity, and mass change were measured during incubation.

Ultrasonic measurements were performed using the Ultrasonic Measuring System UZP-1 (INCO- VERITAS) with enhanced accuracy of the time of transmission of ultrasonic waves (±0.01 μs). A pulse ultrasonic technique was used to determine the elastic properties: Young's modulus (E) and Kirchoff's modulus (G), and Poisson's ratio (μ). A 10-MHz transducer with a diameter of 10 mm and connected to a sample by paraffin oil was used for longitudinal waves and the same transducer was glued to the samples using Canadian balm for transverse waves. Values of the material constants were calculated using the following formula:

$$E = C_L^2 \cdot \rho \cdot \frac{(1+\mu)\cdot(1-2\mu)}{(1-\mu)} \quad (2)$$

$$E = 2G(1+\mu) \quad (3)$$

where: E = Young's modulus, G = Kirchhoff's modulus, μ = Poisson's ratio, ρ = apparent density, and C_L = speed of a longitudinal wave.

Mechanical tests were carried out using a Tira Test 2200 machine in the compressive mode at an upper-crosshead speed of 2 mm/min at ambient temperature according to the ISO 844:1993: DIN 53420 standard. Samples were prepared according to the PN-EN ISO 604 standard as a cylinder with a 10-mm diameter and 10-mm height. The reported mechanical properties were calculated by averaging measurements of the three specimens.

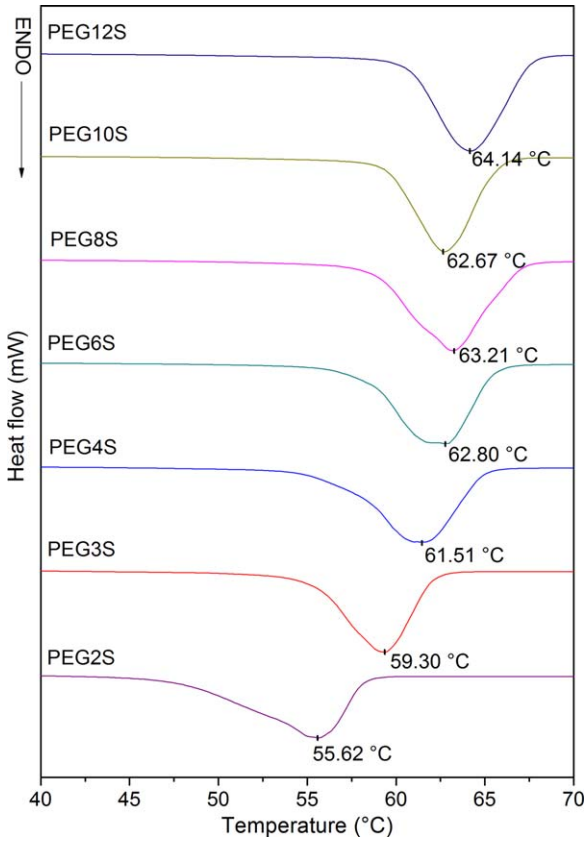

Figure 1. DSC curves of PEG/starch systems. [Color figure can be viewed in the online issue, which is available at wileyonlinelibrary.com.]

RESULTS AND DISCUSSION

Investigation of PEG/Starch Systems

In the first step, the PEG/starch systems were investigated using DSC. Figure 1 shows the DSC curves of PEG with different molecular weights and stabilized with potato starch and the melting temperatures, which were determined from the DSC curves as a peak minimum.

The temperature of phase transition was in the range of 55.6–64.1 °C, and it had a tendency to increase with increasing PEG molecular weight. The results obtained are in good agreement with the literature values reported for PEG.[16]

Additionally, using the DSC data (Figure 1), the heat of phase transition (ΔH_m) was determined, and the degree of crystallinity (X_c) was calculated using the formula (4):

$$X_c = \frac{\Delta H - \Delta H_a}{(1-x)\Delta H_m^0} \cdot 100\% = \frac{\Delta H_m}{(1-x)\Delta H_m^0} \cdot 100\% \quad (4)$$

where: ΔH_m^0 = heat of melting of 100% crystalline polymer (196.8 J/g for PEG),[25] ΔH_m = heat of melting of polymer under investigation determined by DSC, and x = starch content in the SSPCM. The results are shown in Table I.

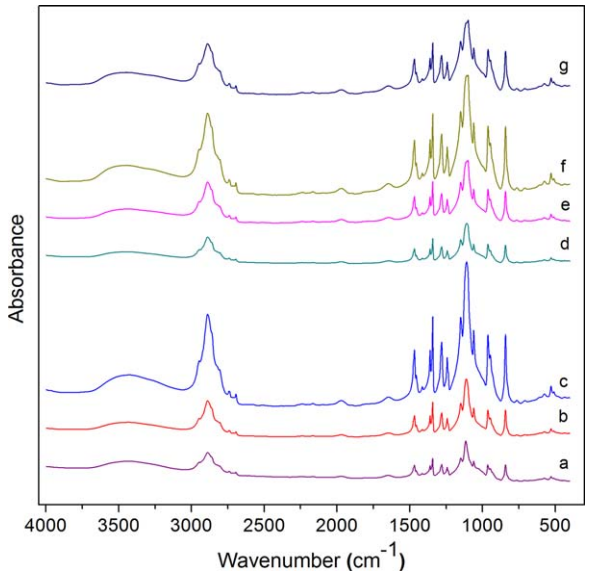

Figure 2. FTIR spectra of PEG/starch systems: (a) PEG2S, (b) PEG3S, (c) PEG4S, (d) PEG6S, (e) PEG8S, (f) PEG10S, and (g) PEG12S. [Color figure can be viewed in the online issue, which is available at wileyonlinelibrary.com.]

The DSC analysis showed that the PEG/starch systems undergo endothermic phase transition, and the temperature of phase transition was slightly lower than that of pristine PEG. The most promising SSPCMs were systems containing PEG 4000, PEG 8000, and PEG 12,000 because they had the highest melting heat and degree of crystallinity (>90%). Generally, PEGs are semicrystalline polymers which, in the solid state, contain both amorphous and crystalline regions in varying proportions depending upon the synthesis, molar mass, dispersity, and their thermal history.[26,27] In the amorphous phase, the polymer chains have a random orientation, while in the crystalline regions, PEG chains exist as a double parallel helix.[28,29] The helices are arranged as plate-like structures known as lamellae from which the hydroxyl end-groups are rejected onto the surfaces and finally, lamellae form often large and well-formed spherulites.[30,31] It was found that the critical value of PEG molecular mass was around 4000, and that polymers with lower molecular mass fractions (MW < 4000) crystallize in the form of extended chains with a melting point of about 56 °C, and the higher molecular mass fractions (MW > 4000) crystallize as folded chains with a melting point in the range 65–70 °C.[19,32] For PEG with an average molar mass in the range 2500–4000, a double melting peak is usually observed.[32] However, as can be seen from the DSC profiles in the studied PEG/starch systems, the shape of the peaks suggests that there are two overlapping phase-transition peaks. This effect can be attributed to the hydrogen bonds in SSPCM, which cause both nucleation and growth of PEG crystals; however, both processes are significantly influenced by the morphology of the existing starch structures. The first peak evidences the phase transition of PEG under confinement in the starch grains, and the second refers to the phase transition of PEG in the bulk phase. The heat effect depends on the amount of PEG confined in the starch grains, which influences morphological features of the starch's hierarchical structures. In the area of poly(ethylene oxide) (PEO) confined systems, He *et al.*[33] investigated the fractional crystallization behavior of PEO confined in various pre-existing poly (butylene succinate) crystals. They concluded that the crystallization of PEO was dependent not only on the local concentration and segregations of PEO, but also on the intrinsic morphological features of poly(butylene succinate) spherulites. A decrease of PEG melting temperature under confinement was also observed during crystallization of PEO confined in narrowly distributed, stable nanodroplets. The authors found that nucleation in these PEO droplets occurs only at high supercooling, and that the polymer structure in the crystallized droplets is topologically controlled with a loosely layered lamellar structure.[34] This effect was also observed in PEO/fatty acid blends.[35] The FTIR spectra of the PEG/starch systems are presented in Figure 2.

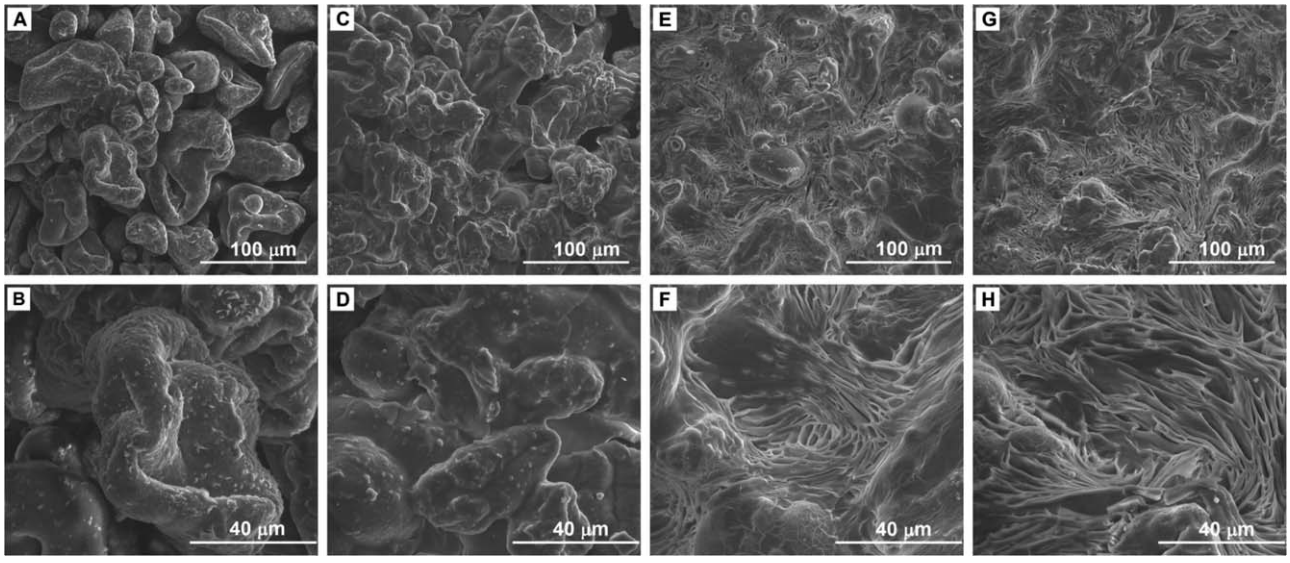

Figure 3. SEM images of PEG/starch systems: (A,B) PEG2S, (C,D) PEG4S, (E,F) PEG8S, and (G,H) PEG12S.

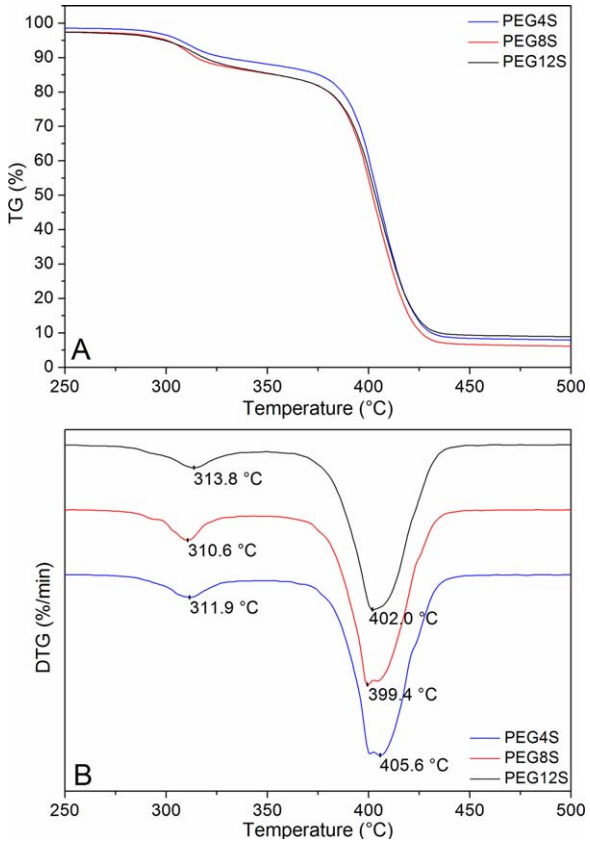

Figure 4. TG (A) and DTG profiles (B) of PEG/starch systems. [Color figure can be viewed in the online issue, which is available at wileyonlinelibrary.com.]

The broad peaks at 3425–3453 cm^{-1} are related to the O—H stretching vibrations. The triplet peak at 1060–1151 cm^{-1} is associated with the C—O—C stretching vibrations, which are characteristic for the PEG spectrum. For the PEG of lower molecular weights (2000–6000), the triplet has one maximum, and the peak moved toward lower wavenumbers with increasing molecular weight of PEG. For PEG of higher molecular weight (>6000), the maximum of the triplet peak was divided into two peaks (1108 and 1100 cm^{-1}), which was probably due to the partial encapsulation of PEG chains inside the starch grains, as can be observed in the SEM microphotographs (Figure 3). With increasing PEG molar mass, larger amounts of PEG are observed outside the starch grains and the C—O bands lie in a region similar to that of pure PEG.[35] The peaks at 2947, 2890, 2741, 1467, and 1281 cm^{-1} are characteristic for CH_2 stretching.[27] The peak occurring at 764 cm^{-1} corresponds to C—C stretching vibrations. The position of peaks belonging to O—H and C—O—C functional groups depends on the molecular weight of PEG.

In the PEG/starch blends, hydrogen bonds between OH groups from amylose/amylopectin and ether oxygens from PEG macrochains can be formed, which is evidenced by a shift of the characteristic bands of both the O—H groups (proton-donor groups) and C—O as the proton-acceptor groups. It was found that for PEG with a lower molar mass in the PEG/starch systems, the peak from the O—H stretching vibration bands was in the region 3432–3425 cm^{-1}, which is at larger wavenumbers than for pure potato starch.[22,36] For systems with higher molar mass of PEG, this peak was shifted to higher wavenumbers (up to 3453 cm^{-1} for PEG10S), and this effect can be attributed to a decrease of PEG/starch hydrogen interactions due to fact that longer chains of PEG are located partially outside of the starch grains. Hydrogen bonds between starch and PEG that were probably formed during the starch gelatinization process in the presence of PEG play a fundamental role in the shape stabilization of PCM.[22]

The presence of starch strongly influences PEG morphology as shown in Figure 3. For the PEG2S blend [Figure 3(A,B)], starch grains of different sizes and showing sharp boundaries were visible. For the PEG4S composite [Figure 3(C,D)], the grains were aggregated and there were no sharp boundaries between them. On the surface of grains for PEG2S and PEG4S samples, fine crystallites of PEG were located. The microstructure of composites containing higher molecular weight PEG [PEG8S and PEG12S—Figure 3(E–H)] was dominated by polyether crystal structures with numerous small starch grains. It seems that the longer PEG chains are not able to enter the starch grains and they crystallize outside in the bulk. Therefore, the PEG component can efficiently absorb the cement heat of polymerization while keeping its shape due to the formation of hydrogen bonds with amylose/amylopectin.

The thermal stability of PEG/starch modifiers for acrylic bone cements was investigated using the TG method under non-isothermal conditions, and the results are presented in Figure 4 and Table II.

From the obtained mass-loss profiles, it can be seen that PEG stabilized with potato starch remains stable up to about 280 °C, and the degradation process occurs in two steps with a maximum rate at 310 °C and 400 °C. Additionally, in the first peak, which comes from the starch degradation, two shoulders were visible. A similar effect was observed by Janković[37] in cassava starch, where it was found that the main degradation step at about 300–350 °C was accompanied by an additional sub-step. Degradation in this temperature range proceeds through a series

Table II. TG Results for PEG/Starch Systems

Sample	$T_{1\%}$ (°C)	$T_{3\%}$ (°C)	$T_{5\%}$ (°C)	$T_{10\%}$ (°C)	$T_{20\%}$ (°C)	$T_{50\%}$ (°C)	Char residue at 550 °C (%)
PEG4S	292	305	312	345	389	405	7.59
PEG8S	288	303	309	328	385	403	5.61
PEG12S	284	302	310	331	385	404	8.34

Table III. Setting Times of Acrylic Bone Cement (Gillmore Needle Method)

	Setting time				
Sample	Initial setting time (t_I)	Final setting time (t_F)	T_{max} (°C)	T_{set} (°C)	t_{set}
Pure cement	12 min 30 s	13 min	70.2	46.08	10 min 45 s
C_PEG2S	13 min 40 s	14 min 10 s	60.0	40.98	13 min 50 s
C_PEG3S	13 min 50 s	14 min 30 s	63.5	42.73	13 min 25 s
C_PEG4S	13 min	13 min 20 s	62.5	42.23	13 min 26 s
C_PEG6S	9 min 50 s	10 min 40 s	62.5	42.23	10 min 07 s
C_PEG8S	12 min 40 s	13 min 30 s	58.3	40.13	11 min 25 s
C_PEG10S	13 min 30 s	14 min 20 s	63.4	42.68	13 min 53 s
C_PEG12S	14 min 10 s	14 min 40 s	60.2	41.08	14 min 05 s

Curing parameters: maximum temperature (T_{max}), the setting temperature (T_{set}), and the setting time (t_{set}) of acrylic bone cement modified with PEG/starch systems.

of competitive reactions, which include free-radical depolymerization via chain scission of the glycosidic linkage of polysaccharide, and subsequent decomposition of amylopectin and amylase degradation products. The second peak can be attributed to the degradation of PEG,[38] which undergoes thermal decomposition in one main degradation step through chain scission. However, as can be seen from the DTG curves, two overlapping peaks can be seen at about 400–420 °C, and the second peak intensity increased with increasing PEG molecular weight. This effect can probably be attributed to altered degradation pathways of PEG under confinement in the starch grains and the bulk PEG outside the granules. As can be seen in the SEM microphotographs, with increasing PEG molar mass, the amount of PEG outside of the starch granules also increases. It is noteworthy that in the work by Barroso-Bujans *et al.*,[39] where thermal degradation of PEO composites with graphene oxide was investigated, the authors found that PEO intercalated and under confinement decomposed at lower temperatures than neat PEO, while the excess of PEO phase in PEO–graphene oxide composites underwent degradation at temperatures close to that of neat PEO.

To summarize the thermal analysis section, PEG/starch blends are stable up to 280 °C. Since the polymerization temperature of acrylic bone cement is about 70 °C, one can safely apply PEG/starch systems as cement modifiers.

Investigation of Acrylic Bone Cements Modified with PEG/Starch Blends

The influence of the SSPCM content on the setting time of acrylic bone cement is shown in Table III. Pure acrylic bone cement had initial and final setting times of ~12 min 30 s and 13 min, respectively. Bone cements modified with PEG/starch systems showed generally longer initial and final setting times than the pure cement. The initial setting time was from 30 s to 2 min longer than for pure cement, and the setting process took 20–50 s more in comparison with the pristine cement. Only the C_PEG6S system was characterized by shorter initial and final setting times than the other bone cements ($t_I = 9$ min 50 s, $t_F = 10$ min 40 s).

The curing process of acrylic bone cement modified with SSPCM was delayed in comparison to the pure cement. The heat liberated during the polymerization reaction is partially absorbed by the endothermic effect of the PEG/starch phase transition; consequently, the maximum temperature of the bone cement is reduced.

There is no clear relationship between molecular weight of PEG and the setting time of bone cement. Despite the fact that the setting time of modified bone cements was longer or shorter than that of pure cement, the setting time is still compliant with the ISO 5833:2002 standard, which defines that the setting time should be between 3 and 15 min.[40] To verify the setting time obtained using the Gillmore method and to measure the polymerization temperature of acrylic bone cement, temperature measurements as a function of time were made by applying a thermocouple. Based on temperature–time profiles, parameters such as setting time, curing temperature, and the maximum temperature were obtained.

Figure 5 shows the temperature–time profiles obtained for all investigated cements. The ambient temperature (T_{amb}) was determined as an arithmetic mean of the initial temperatures of all cements and it was 21.96 ± 0.86 °C.

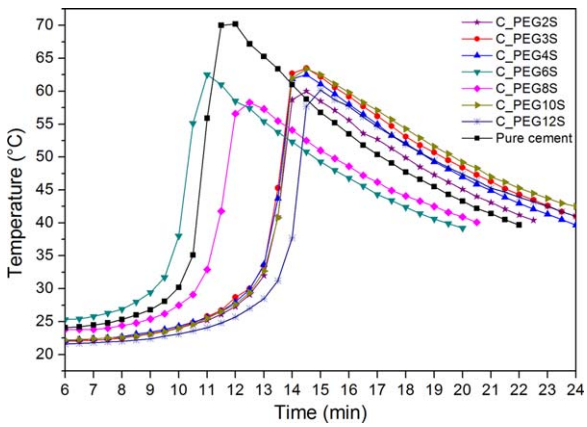

Figure 5. Polymerization exotherms of acrylic bone cement modified with PEG/starch blends. [Color figure can be viewed in the online issue, which is available at wileyonlinelibrary.com.]

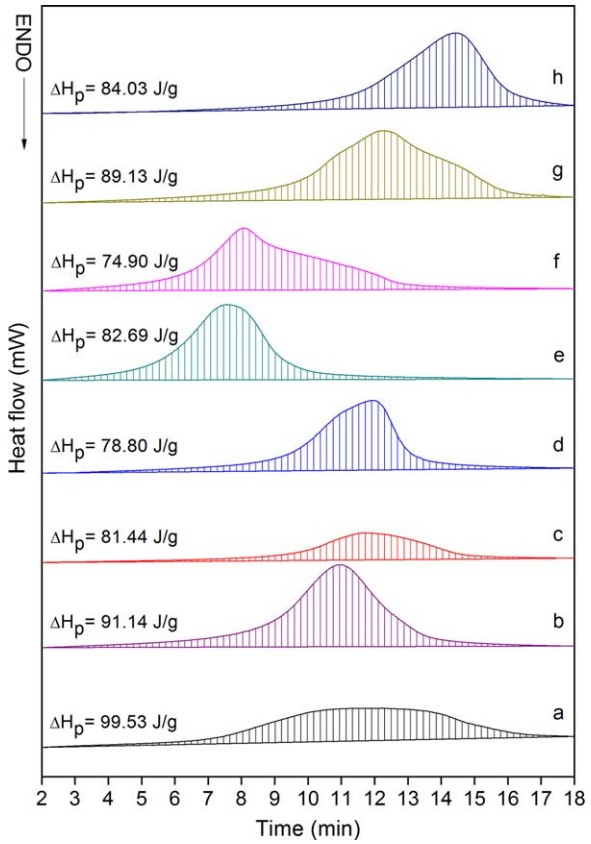

Figure 6. DSC curves of acrylic bone cement modified with PEG/starch systems: (a) pure cement, (b) PEG2S, (c) PEG3S, (d) PEG4S, (e) PEG6S, (f) PEG8S, (g) PEG10S, and (h) PEG12S); heat of polymerization (ΔH_p). [Color figure can be viewed in the online issue, which is available at wileyonlinelibrary.com.]

The curing parameters—the maximum temperature (T_{max}), the setting temperature (T_{set}), and the setting time (t_{set})—obtained from the temperature–time profiles are given in Table III. The maximum temperature of pure cement was 70.2 °C. A decrease in the maximum temperature of modified bone cements from 6.7 °C to 11.9 °C was observed and depended on the molecular weight of PEG. The largest temperature decrease was recorded for cement containing PEG 8000 (C_PEG8S). For this blend, a decrease of 11.9 °C in the maximum temperature and an increase of 40 s in the setting time were found.

The thermal profiles of the polymerization process of acrylic bone cement modified with PEG/starch shown in Figure 5 reveal that the process' autoacceleration due to the Trommsdorff (or "gel") effect[41,42] is generally retarded by the PCM.

Next, the DSC technique was used to study the amount of heat released during the polymerization reaction of bone cements. DSC curves and values of the heat of the polymerization reaction are shown in Figure 6.

The DSC results confirmed that the addition of SSPCM resulted in a decrease in the heat of polymerization for all modified cements, and the lowest heat of polymerization was displayed by acrylic bone cement containing PEG 8000. It was found that the pure cement released the highest amount of heat of polymerization (99.53 J/g) and incorporation of PEG lowered this value. The most promising cement modifiers were systems containing PEG 8000 and PEG 4000 as the smallest amount of heat was released. As can be seen in Table I, the highest heat of phase transition was observed for PEG12S, PEG4S, and PEG8S, and the temperature range of the phase transition depends on the molar mass of PEG. However, it seems that the phase-transition range for PEG4S and PEG8S is more suitable to accumulate thermal energy released during cement polymerization, as the heat of polymerization was lower for PEG4S and PEG8S than that of PEG12S. This proves that the temperature range of phase transition has to correspond to the temperature range of the cement curing process to effectively store the heat generated during the curing process.

The SEM micrographs of acrylic bone cements are shown in Figure 7. The PMMA microspheres of 5–40 μm diameter can be seen in all materials.

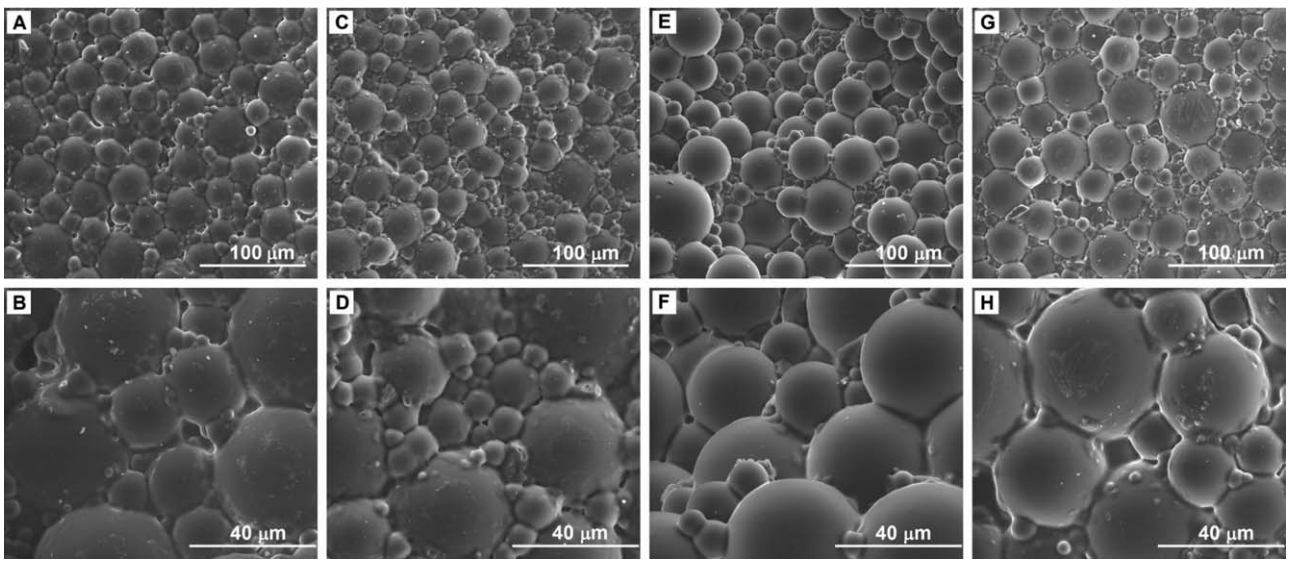

Figure 7. SEM images of acrylic bone cements modified with PEG/starch material: (A,B) unmodified cement, (C,D) C_PEG4S, (E,F) C_PEG8S, and (G,H) C_PEG12S.

Table IV. The Mass of Samples before and 2 Days after Incubation

Sample	Initial mass (g) before incubation	Final mass (g) after incubation	Mass change (%)
Pure cement	3.630	3.717	2.40
C_PEG2S	3.522	3.646	3.52
C_PEG3S	3.682	3.853	4.64
C_PEG4S	3.370	3.505	4.01
C_PEG6S	3.724	3.890	4.46
C_PEG8S	3.391	3.881	14.45
C_PEG10S	3.809	4.015	5.41
C_PEG12S	3.708	3.817	2.94

Growth of the PMMA microspheres was observed in the presence of PEG with higher molecular weights, which might be associated with the retardation in the kinetics of the polymerization reaction caused by the temperature decrease due to heat absorption by the PCM.

Important information can be gained from incubation studies. The protocol involved weighing the pristine composites before and after incubation. The results (Table IV) show that the mass of all samples was increased after 3 months of incubation. The smallest increase of 2.4% was recorded for pure cement and the largest increase (14.45%) for the C_PEG8S sample.

During the incubation period, the incubation fluid was analyzed every week for pH and conductivity. Initially, the incubation fluid had a pH in the range 6.44–6.95, and the highest pH of 6.8 was observed for pure cement. For PEG/starch systems, the solution became more acidic, reaching a final pH value of about 5.2. This effect can be associated with starch degradation through a hydrolysis reaction[43] and as a result, glucose, other sugars, non-sugar compounds, and acids are formed.

The incubation fluid conductivity showed considerable changes during the first 5 weeks of incubation, similar to the pH changes. After this period, the conductivity of incubation liquids was relatively stable. The highest conductivity was reached for pure cement incubation fluid (ca. 35 μS) and the lowest came from C_PEG3S and C_PEG4S blends. For the C_PEG8S material, the changes in incubation fluid conductivity were the most similar to the pure cement.

Mass gain of samples due to the incubation process is probably the result of the water absorption into the pores, which were formed in the samples due to elution of the PEG/starch systems. The pH values and the conductivity reached finally a plateau, what is a proof for material stability at 37 °C. A slight decrease in pH values of modified cements might be a result of the presence of starch in the samples.

Taking into account the potential applications of bone cements, determination of the materials' characteristics and mechanical properties before and after incubation is of primary importance. In this context, the ultrasonic testing method is a useful tool for characterization of the composites' homogeneity and the elasticity of the investigated materials.

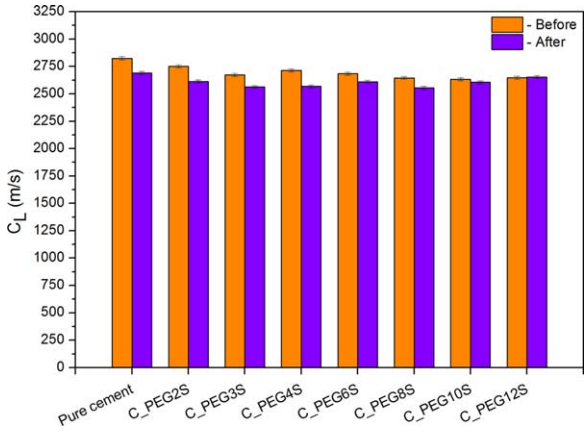

Figure 8. Longitudinal wave speed (C_L) of acrylic bone cement modified with PEG/starch material before and after incubation. Error bars represent standard deviation. [Color figure can be viewed in the online issue, which is available at wileyonlinelibrary.com.]

First, propagation speed of longitudinal waves C_L (m/s) was determined (Figure 8).

The propagation speed was the highest for pure cement compared to modified materials, and it was lower for samples after incubation. Generally, the lower propagation speed of

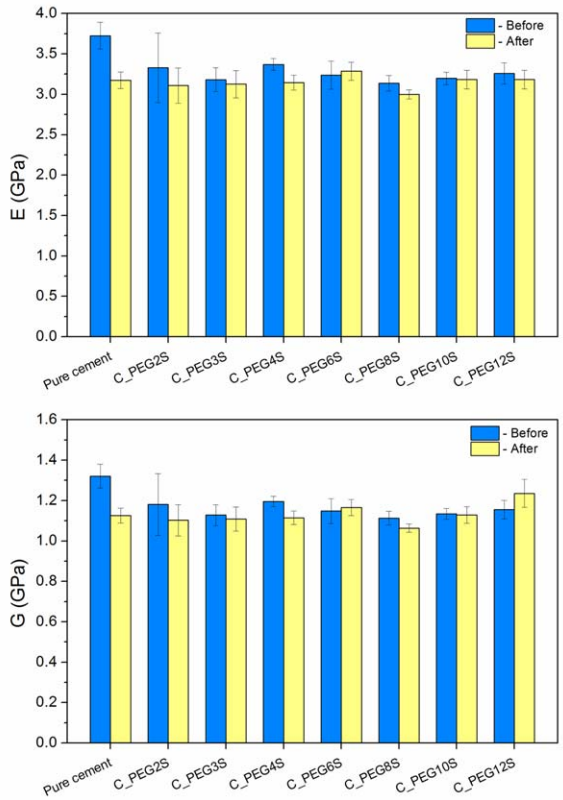

Figure 9. Theoretical Young's modulus E (GPa) and Kirchoff's modulus G (GPa) calculated based on measurements of ultrasound velocities for Poisson's ratio $\mu = 0.41$. Error bars represent standard deviation. [Color figure can be viewed in the online issue, which is available at wileyonlinelibrary.com.]

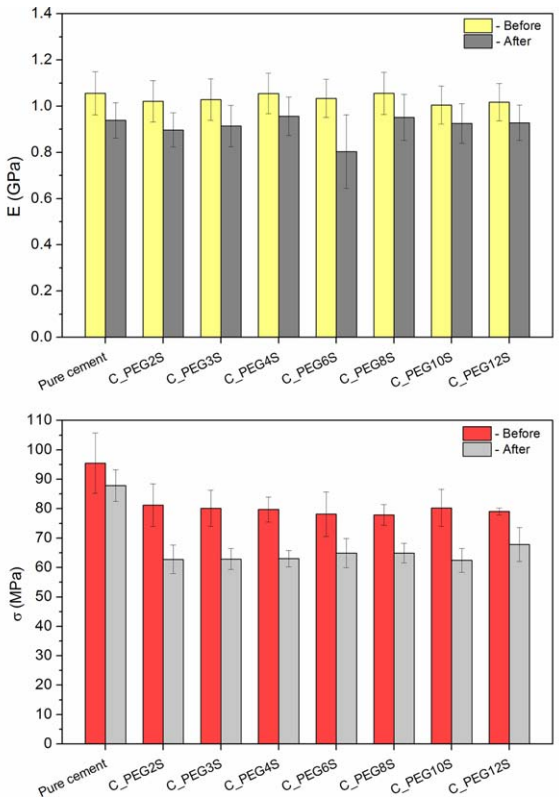

Figure 10. Young's modulus E (GPa) and compressive strength σ (MPa) for compression of acrylic bone cement modified with PEG/starch material before and after incubation. Error bars represent standard deviation. [Color figure can be viewed in the online issue, which is available at wileyonlinelibrary.com.]

longitudinal waves, the less homogeneous the material was. Due to the ultrasonic waves dispersion on defects, grain boundaries, and pores, their velocity falls when a material is non-homogeneous.[44] Ultrasonic analysis showed that modified bone cements are, due to incorporation of the PEG/starch component, less homogeneous than the pure cement. This is in accordance with morphological characteristics of modified cements by the SEM method. A decrease in the propagation speed after incubation confirmed the formation of material defects (pores, cracks, voids, etc.) due to water activity.

The values of density of the cement materials before and after incubation, based on ultrasonic analysis, were calculated. The density of acrylic bone cements was in the range 1.0–1.1 g/cm^3, and for modified blends it was higher after incubation as compared with non-incubated materials. The opposite trend was found for pure cement due to water migration toward the hydrophilic PEG/starch systems. Even after a long drying time, some amount of water remains in the composite material, which is manifested by a mass increase after incubation (Table IV).

Based on the above results, the theoretical Young's modulus E (GPa) and Kirchhoff's modulus G (GPa) were calculated using the Poisson's ratio ($\mu = 0.41$) for SSPCMs. For PMMA, the Poisson's ratio was assumed as 0.4,[45] and for PEG and starch as 0.5[46,47]; the percentage of SSPCM in final cured cement was 10 wt %. The results are presented in Figure 9. Before incubation, the pure cement samples had the highest Young's modulus and Kirchhoff's modulus. Most of samples (except C_PEG6S and C_PEG12S) had lower E and G values after incubation. Addition of the PEG/starch component caused a slight decrease in both the E and G moduli, but their values were still in the range of unmodified cement before and after incubation.

A classical compression test was then performed to determine the compressive strength of modified acrylic bone cements. The average compressive strength data of incubated cements, before and after the incubation process, are presented in Figure 10.

Pure bone cement had a higher compressive strength and there was no significant impact of incubation on this mechanical parameter. However, the addition of PEG/starch systems caused a decrease in the compressive strength values. For modified

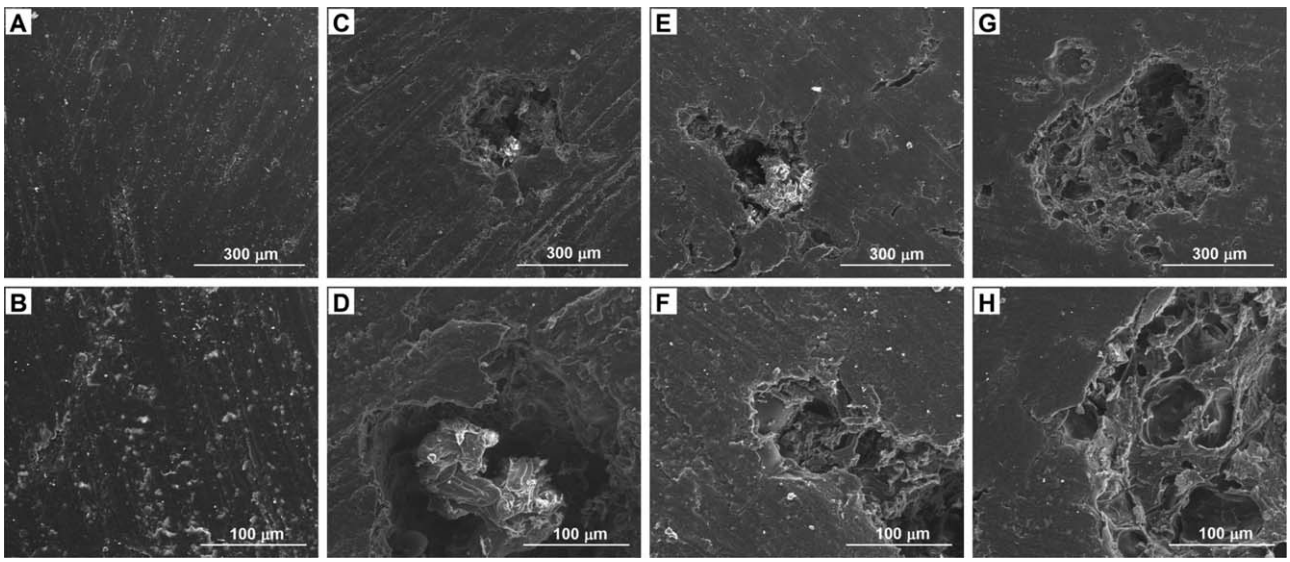

Figure 11. SEM microphotographs of the surface of acrylic bone cements modified with PEG/starch material: (A,B) unmodified cement, (C,D) C_PEG4S, (E,F) C_PEG8S, and (G,H) C_PEG12S after incubation.

bone cements, the compressive strength decreased from 80 MPa to 60 MPa on average due to the incubation process. According to the ISO 5833 standard, the minimum requirement for compression strength is 70 MPa[48] and, before incubation, all investigated cements had a compression strength of above 70 MPa. The strength loss that occurred after incubation could be caused by dissolving PEG in water and the starch degradation. As a result, tiny pores are formed on the sample surface (Figure 11), the material loses its integrity and consequently, a decrease in the compressive strength is observed.

For unmodified cement, a pore-free surface can be observed, but for acrylic bone cements modified with PEG/starch, pores are formed and their size is in the range 100–400 μm. This pore size favours cell proliferation in the process of bone formation.[49]

Analogous effects of a decrease in the compressive strength after incubation were also observed by other authors.[50,51] On the other hand, the pores can be occupied in the regeneration process by freshly grown bone tissue and, as a result, the final mechanical strength of bone cement will increase. This effect was observed by He *et al.*[52] for PMMA-based bioactive bone cements consisting of bioactive glass and chitosan. A porous surface structure obtained by the degradation of the chitosan promoted bone ingrowth and improved the interfacial bonding strength, thus resulting in better mechanical properties.

CONCLUSIONS

In this work, the influence of a shape-stabilized phase-change material consisting of PEG of different molecular weights and potato starch on the structure and morphology of acrylic bone cement was investigated. Thermal and mechanical properties were also examined. The results showed that the addition of 15% PEG/starch blend leads to a significant decrease in the maximum polymerization temperature from 70 °C for unmodified cement to 58 °C for PEG/starch-modified cement. The heat capacity of PEG/starch systems depended on the molecular weight and the degree of crystallinity of PEG. The best results were obtained for PEG 8000, but PEG 4000 and PEG 12,000 also showed promising features. TG analysis proved that the PEG/starch systems have good thermal stability, which is important due to storage and use requirements. The compressive strength of modified bone cements was lower than that for pure cement, but still fulfilled the requirements of the appropriate ISO standard. The investigated materials showed good stability in incubation tests, although a decrease in the propagation speed after incubation confirmed the formation of material defects (pores, cracks, voids, etc.) due to water activity. However, these defect sites can be occupied in the regeneration process by freshly grown bone tissue and, as a result, the final mechanical strength of bone cement will even increase.

In our previous work, we investigated the influence of pure PEG on the thermal and mechanical properties of acrylic bone cement.[53] The pristine PEG worked as a more efficient heat accumulator but due to PEG leakage significant mechanical strength loss was observed. Therefore, the shape stabilization is necessary and in future works we are going to analyze other polymeric materials as shape stabilizers for PEG.

ACKNOWLEDGMENTS

The authors are grateful to the Statutory Fund of AGH University of Science and Technology, Faculty of Materials Engineering and Ceramics (contract no. 11.11.160.616). Kinga Pielichowska acknowledges financial support from the National Science Centre in Poland (grant no. DEC-2011/03/B/ST8/05255).

REFERENCES

1. Yang, D.; Yoon, G.; Shin, G.; Kim, S.; Rhee, J.; Khang, G.; Lee, H. *Macromol. Res.* **2015**, *13*, 120.
2. Hamid, R. S. H.; Mohammad, E.; Farivarabdollahzadeh, L.; Ali, S. S.; Aidin, M.; Sina, E. In Arthroplasty; Kinov, P., Ed.; InTech: Croatia, **2013**; Chapter 5, p 101.
3. Kuehn, K. D.; Ege, W.; Gopp, U. *Orthop. Clin. North Am.* **2005**, *36*, 17.
4. Yang, J. M. *Biomaterials* **1997**, *18*, 1293.
5. Beck, S.; Boger, A. *Acta Biomater.* **2009**, *5*, 2503.
6. Charnley, J. *Br. J. Surg.* **1970**, *57*, 874.
7. Charnley, J. *J. Bone Joint Surg. Br. B* **1960**, *42*, 28.
8. Boesel, L. F.; Reis, R. L. *Prog. Polym. Sci.* **2008**, *33*, 180.
9. Hagan, C. P.; Orr, J. F.; Mitchell, C. A.; Dunne, N. J. *J. Mater. Sci. Mater. Med.* **2009**, *20*, 2427.
10. Zhang, H.; Brown, L.; Blunt, L. *J. Mater. Sci. Mater. Med.* **2008**, *19*, 591.
11. Farrar, D. F.; Rose, J. *Biomaterials* **2001**, *22*, 3005.
12. Dunne, N. J.; Orr, J. F. *J. Mater. Sci. Mater. Med.* **2002**, *13*, 17.
13. Liptakova, T.; Lelovics, H.; Necas, L. *Acta Bioeng. Biomech.* **2009**, *11*, 47.
14. Dipisa, J. A.; Sih, G. S.; Berman, A. T. *Clin. Orthop. Relat. Res.* **1976**, *121*, 95.
15. Pascual, B.; Gurruchaga, M.; Ginebra, M. P.; Gil, F. J.; Planell, J. A.; Vázquez, B.; San Román, J.; Goñi, I. *Biomaterials* **1999**, *20*, 453.
16. Ormsby, R.; McNally, T.; Mitchell, C.; Halley, P.; Martin, D.; Nicholson, T.; Dunne, N. *Carbon* **2011**, *49*, 2893.
17. Fadeel, B. Handbook of Safety Assessment of Nanomaterials: From Toxicological Testing to Personalized Medicine; Pan Stanford Publishing: Boca Raton, **2015**.
18. De Santis, R.; Ambrogi, V.; Carfagna, C.; Ambrosio, L.; Nicolais, L. *J. Mater. Sci. Mater. Med.* **2006**, *17*, 1219.
19. Pielichowski, K.; Flejtuch, K. *Polym. Adv. Technol.* **2002**, *13*, 690.
20. Pielichowska, K.; Pielichowski, K. *Prog. Mater. Sci.* **2014**, *65*, 67.
21. Yu, M.; Huang, S.; Yu, K. J.; Clyne, A. M. *Int. J. Mol. Sci.* **2012**, *13*, 5554.
22. Pielichowska, K.; Pielichowski, K. *J. Appl. Polym. Sci.* **2010**, *116*, 1725.

23. Pielichowska, K.; Błażewicz, S. Polish Pat. P.406713, December 11 (**2015**).
24. ASTM C266-99. Standard Test Method for Time of Setting of Hydraulic-Cement Paste by Gillmore Needles; ASTM International: West Conshohocken, PA, **1999**.
25. Polyoxyethylene (POE) Heat Capacity, Enthalpy, Entropy, Gibbs Energy, ATHAS Database. SpringerMaterials Release 2014. Version 2014.06. Editor: M. Pyda. Available at: http://materials.springer.com/polymerthermodynamics/docs/athas_0068 (accessed October 5, **2015**).
26. Buckley, C. P.; Kovacs, A. *J. Colloid Polym. Sci.* **1976**, *254*, 695.
27. Bailey, F. E.; Koleske, J. V. Poly(ethylene oxide); Academic Press: New York, **1976**.
28. Tadokoro, H. *J. Polym. Sci. Macromol. Rev.* **1967**, *1*, 119.
29. Takahashi, Y.; Tadokoro, H. *Macromolecules* **1973**, *6*, 672.
30. Kovacs, A. J.; Gonthier, A.; Straupe, C. *J. Polym. Sci. Polym. Symp.* **1975**, *50*, 283.
31. Bailey, F. E.; Koleske, J. V. *J. Chem. Educ.* **1973**, *50*, 761.
32. Sánchez-Soto, P. J.; Ginés, J. M.; Arias, M. J.; Novák, C.; Ruiz-Conde, A. *J. Therm. Anal. Calorim.* **2002**, *67*, 189.
33. He, Z.; Liang, Y.; Han, C. C. *Macromolecules* **2013**, *46*, 8264.
34. Taden, A.; Landfester, K. *Macromolecules* **2003**, *36*, 4037.
35. Pielichowska, K.; Gkowinkowski, S.; Lekki, J.; Binias, D.; Pielichowski, K.; Jenczyk, J. *Eur. Polym. J.* **2008**, *44*, 3344.
36. Kizil, R.; Irudayaraj, J.; Seetharaman, K. *J. Agric. Food Chem.* **2002**, *50*, 3912.
37. Janković, B. *Carbohydr. Polym.* **2013**, *95*, 621.
38. Pielichowski, K.; Flejtuch, K. *J. Anal. Appl. Pyrol.* **2005**, *73*, 131.
39. Barroso-Bujans, F.; Alegría, A.; Pomposo, J. A.; Colmenero, J. *Macromolecules* **2013**, *46*, 1890.
40. Lewis, G.; Xu, J.; Madigan, S.; Towler, M. R. *Acta Biomater.* **2007**, *3*, 970.
41. Norrish, R. G. W.; Brookman, E. F. *Math. Phys. Sci.* **1939**, *171*, 147.
42. Trommsdorff, V. E.; Köhle, H.; Lagally, P. *Makromol. Chem.* **1948**, *1*, 169.
43. Pappas, C. A. Starch Hydrolysis by Heating in Hermetically Sealed Systems at Neutral pH; Kansas State University: Manhattan, Kansas, **1963**.
44. Lionetto, F.; Montagna, F.; Maffezzoli, A. *Appl. Rheol.* **2005**, *15*, 326.
45. Proulx, T. Mechanics of Time-Dependent Materials and Processes in Conventional and Multifunctional Materials; Springer: Bethel, Connecticut, **2011**; Vol.*3*.
46. Ma, P. X.; Elisseeff, J. Scaffolding in Tissue Engineering; CRC Press: Boca Raton, **2005**.
47. Bahat, D.; Rabinovitch, A.; Frid, V. Tensile Fracturing in Rocks: Tectonofractographic and Electromagnetic Radiation Methods; Springer: Berlin, **2005**.
48. Lilikakis, A.; Sutcliffe, M. P. F. *Int. Orthop.* **2009**, *33*, 815.
49. Murphy, C. M.; Haugh, M. G.; O'Brien, F. J. *Biomaterials* **2010**, *31*, 461.
50. Kühn, K. D.; Specht, R.; Ege, W.; Kock, H. J. In Bone Cements and Cementing Technique; Walenkamp, G. H. I. M.; Murray, D. W.; Henze, U.; Kock, H. J., Eds.; Springer: Berlin Heidelberg, **2001**; Chapter 4, p 27.
51. Canul-Chuil, A.; Vargas-Coronado, R.; Cauich-Rodríguez, J. V.; Martínez-Richa, A.; Fernandez, E.; Nazhat, S. N. *J. Biomed. Mater. Res. Part B: Appl. Biomater.* **2003**, *64*, 27.
52. He, Q.; Chen, H.; Huang, L.; Dong, J.; Guo, D.; Mao, M.; Kong, L.; Li, Y.; Wu, Z.; Lei, W. *PLoS One* **2012**, *7*, e42525.
53. Król, K.; Pielichowska, K. *Polym. Adv. Technol.* **2016**, DOI: 10.1002/pat.3792.